# Lanthanide(III) Squarates
## 2. High Diversity of Rare Coordination Modes of the Squarate Anion in a Series of Weakly Hydrated Cerium(III) Squarates Prepared by Pseudo-hydrothermal Methods

JEAN-CHRISTIAN TROMBE*, JEAN-FRANCOIS PETIT and ALAIN GLEIZES

*Laboratoire de Chimie de Coordination du CNRS, Unité Propre n. 8241 liée par conventions à l'Université Paul Sabatier et à l'Institut National Polytechnique de Toulouse, 205 route de Narbonne, F-31077 Toulouse Cédex (France)*

(Received March 3, 1989; revised July 31, 1989)

### Abstract

A series of low water content cerium(III) squarates were produced by pseudo-hydrothermally treating the compound $Ce_2(H_2O)_{11}(C_4O_4)_3 \cdot 2H_2O$ (**1**-Ce) in water in a closed vessel. They are: $[Ce(H_2O)_2]_2(C_4O_4)_3$ (**1a**-Ce), $[Ce(H_2O)_2]_4(C_4O_4)_6 \cdot 3H_2O$ (**1b**-Ce) and $[Ce,Ce(H_2O)_2]_2(OH)_2(C_4O_4)_5 \cdot 0.6H_2O$ (**1c**-Ce). The crystal structures were determined by X-ray single crystal techniques. **1a**-Ce: monoclinic, space group $P2_1/c$, $a = 7.143(1)$, $b = 16.940(4)$, $c = 6.994(1)$ Å, $\beta = 101.24(2)°$, $V = 830$ Å$^3$, $Z = 2$; **1b**-Ce: triclinic, space group $P\bar{1}$, $a = 7.579(1)$, $b = 8.921(2)$, $c = 7.054(1)$ Å, $\alpha = 105.06(2)$, $\beta = 94.02(1)$, $\gamma = 89.94(2)°$, $V = 459$ Å$^3$, $Z = 1$; **1c**-Ce: triclinic, space group $P\bar{1}$, $a = 8.066(1)$, $b = 12.992(1)$, $c = 7.100(2)$ Å, $\alpha = 96.96(1)$, $\beta = 105.15(1)$, $\gamma = 105.93(1)°$, $V = 676$ Å$^3$, $Z = 1$. The squarate anion presents various unusual coordination modes, including chelation, resulting in cerium–oxygen–cerium double bridges. **1a**-Ce has a layer structure, **1b**-Ce a tunnel structure and **1c**-Ce, that further contains cerium–hydroxo–cerium bridges, has a dense 3-D structure. The structure type **1a**-Ce has been shown to exist also for La, Pr, Nd, Sm and Eu. The thermal behaviours of **1a**-La, **1a**-Ce, **1a**-Pr, **1a**-Nd and **1a**-Sm were studied.

### Introduction

In a previous paper [1], we reported on the characterization, crystal structure determination and thermal analysis of several types of lanthanide squarates as obtained from aqueous solution in an open system. The crystal growing of compounds of the type **1**-Ln ($[Ln_2(H_2O)_{11}(C_4O_4)_3 \cdot 2H_2O]$-type) for the purpose of X-ray investigation was attempted by placing a sample of the cerium derivative in a sealed pyrex glass tube half-filled with water and leaving it in a 30–90 °C thermal gradient during approximately 8 weeks. Small acicular crystals formed that presented an X-ray powder pattern different from that of the starting compound. The new compound was named **1**′-Ce. It was presented in a brief communication [2]. It is renamed **1a**-Ce in the present paper. On the basis of the crystal structure determination it was ascribed the formula $[Ce(H_2O)_2]_2(C_4O_4)_3$ which is markedly water poorer than the starting material, **1**-Ce, of formula $Ce_2(H_2O)_{11}(C_4O_4)_3 \cdot 2H_2O$. This result is consistent with the easy dehydration of **1**-Ce which occurs between 80 and 220 °C as shown by thermal gravimetry analysis (the corresponding DTA sharp peak is at 130 °C) [1]. The formation of **1a**-Ce resulted from both the low water solubility of **1**-Ce and its relative ease of dehydration. The lanthanide high coordination number requirement could no longer be ensured by water molecules but by the oxygen atoms of the squarate ligand which appeared to be chelating as a result of the temperature. This is the main structural feature of **1a**-Ce which was the first example of the squarate anion chelating a inner-transition metal as undoubtedly established from a single crystal X-ray study. The chelation of transition metals by the squarate anion has been claimed several times to interpret spectroscopy data [3]. However single-crystal X-ray structure determinations carried out so far on transition metal squarates showed either no chelation or that chelation had been erroneously postulated [4]. The only undoubtful case of chelation by squarate was that of alkali-earth cations found by Robl *et al.* [5–8].

This result prompted us to look for possibly more dehydrated phases by working at higher temperatures. Two new cerium compounds were obtained. They are referred to as **1b**-Ce and **1c**-Ce. The present paper is devoted to the description of the three compounds **1a**-Ce, **1b**-Ce and **1c**-Ce which were produced in a closed system at various temperatures.

*Author to whom correspondence should be addressed.

0020-1693/90/$3.50 

## Experimental

*Syntheses and Characterization*

$[Ce(H_2O)_2]_2(C_4O_4)_3$ (**1a**-Ce) was obtained as a pure phase by placing 100 mg of powdered **1**-Ce, $Ce_2(H_2O)_{11}(C_4O_4)_3 \cdot 2H_2O$ [1], in a Pyrex glass tube half-filled with water (*c.* 10 ml), sealed under vacuum and maintained in a 30–90 °C gradient for two months.

$[Ce(H_2O)_2]_4(C_4O_4)_6 \cdot 3H_2O$ (**1b**-Ce) and $[Ce,Ce(H_2O)_2]_2(OH)_2(C_4O_4)_5 \cdot 0.6H_2O$ (**1c**-Ce): 100 mg of **1**-Ce [1] and about 15 ml of water were introduced in a pyrex glass test tube placed in a steel container which was tightly closed and maintained at 135 or 180 °C for about 6 weeks. As evidenced by X-ray powder diffraction, **1b**-Ce formed as a pure phase while **1c**-Ce formed as scarce single crystals in a mixture mainly containing **1a**-Ce. Crystals of **1c**-Ce were morphologically different from those of **1a**-Ce and **1b**-Ce; they were differentiated and sorted out under the microscope.

New insights into methods of preparation are documented in the 'Discussion'.

The formulae of **1a**-Ce, **1b**-Ce and **1c**-Ce were deduced from crystal structure determinations.

*Crystal Structure Determinations*

Crystal systems, accurate cell constants, space groups and intensity data were obtained from single crystals mounted on an Enraf-Nonius CAD4 computer-controlled X-ray diffractometer. Crystal data and conditions of intensity measurements are gathered in Table 1. The standard reflections showed no abnormal trend. The data were corrected for Lorentz and polarization effects and, in the case of **1c**-Ce, for absorption and secondary extinction.

The structure determinations were carried out using Patterson and Fourier map techniques and refined applying full-matrix least-squares techniques using a DEC VAX 11-730 computer and programs listed in ref. 9. Throughout the refinements, the minimized functions were $\Sigma w(|F_o| - |F_c|)^2$ where $|F_o|$ and $|F_c|$ are the observed and calculated structure factor amplitudes. Atomic scattering factors and anomalous terms are those of Cromer and Waber [10].

TABLE 1. Experimental crystallographic data for **1a**-Ce, **1b**-Ce and **1c**-Ce

| | **1a**-Ce | **1b**-Ce | **1c**-Ce |
|---|---|---|---|
| Crystal data | | | |
| Crystal system | monoclinic | triclinic | triclinic |
| Space group | $P2_1/c$ | $P\bar{1}$ | $P\bar{1}$ |
| $a$ (Å) | 7.143(1) | 7.579(1) | 8.0656(6) |
| $b$ (Å) | 16.940(4) | 8.921(2) | 12.992(1) |
| $c$ (Å) | 6.994(1) | 7.054(1) | 7.100(2) |
| $\alpha$ (°) | 90 | 105.06(2) | 96.96(1) |
| $\beta$ (°) | 101.24(2) | 94.02(1) | 105.15(1) |
| $\gamma$ (°) | 90 | 89.94(2) | 105.93(1) |
| $V$ (Å$^3$) | 830 | 459 | 676 |
| $Z$ | 2 | 1 | 1 |
| Molecular weight | 688.4 | 706.4 | 612.4 |
| $\rho_{cal}$ (g/cm$^3$) | 2.75 | 2.55 | 3.01 |
| Data collection | | | |
| Scan mode | $\theta$-$\theta$ | $\omega$ | $\theta$-2$\theta$ |
| Take-off angle (°) | 3.25 | 5.4 | 3.1 |
| Max. Bragg angle (°) | 33 | 25 | 30 |
| Scan speed[a] | | | |
| SIGPRE[a] | 0.75 | 0.85 | 0.75 |
| SIGMA[a] | 0.018 | 0.010 | 0.018 |
| VPRE (°/min)[a] | 10 | 6.67 | 10 |
| $T_{max}$ (s)[a] | 60 | 90 | 60 |
| Structure refinement | | | |
| Reflections collected | 3422 | 1596 | 4177 |
| Reflections used | 1999 ($I > 3\sigma(I)$) | 1411 ($I > 2\sigma(I)$) | 3465 ($I > 3\sigma(I)$) |
| Weighting: $w^{-1}$ = | $\sigma^2(F_o) + (0.02F_o)^2 + 1$ | $\sigma^2(F_o) + (0.02F_o)^2 + 1$ | $\sigma^2(F_o) + (0.02F_o)^2 + 1$ |
| $R = \Sigma(\|F_o - F_c\|)/\Sigma F_o$ | 0.024 | 0.025 | 0.019 |
| $R_w = (\Sigma w(F_o - F_c)^2/\Sigma F_o^2)^{1/2}$ | 0.026 | 0.031 | 0.026 |

[a]For definition of parameters see ref. 11.

The non-H atoms (except C atoms in **1b**-Ce) were refined anisotropically. The H atoms of the water molecules coordinated to the cerium atoms could be localized. They were introduced in the refinements as fixed contributors. In either of the **1b**-Ce and **1c**-Ce structures, there appeared non-stoichiometric statistically distributed intervening water molecules that will be discussed later. In the last cycle of refinements the largest (variable shift)/(e.s.d.) ratios were less than 1% and the reliability factors were less than or equal to 3%. They are reported in Table 1 along with the weighting schemes and numbers of variables and observations used. No significant feature appeared in the final difference Fourier maps. The atomic positional parameters are listed in Tables 2, 3 and 4 for **1a**-Ce, **1b**-Ce and **1c**-Ce, respectively. Main bond lengths and angles are displayed in Tables 5, 6 and 7, respectively.

TABLE 2. Atomic positions for **1a**-Ce

| Atom | *x* | *y* | *z* |
|---|---|---|---|
| Ce | 0.25783(3) | 0.07978(1) | 0.00681(3) |
| $O_w(1)$ | 0.1415(5) | 0.1779(2) | 0.2325(5) |
| $O_w(2)$ | 0.4773(4) | 0.0837(2) | 0.3346(5) |
| O(11) | 0.7698(4) | 0.3137(2) | −0.1658(5) |
| O(21) | 0.4013(4) | 0.2121(2) | −0.0562(5) |
| O(31) | 0.6192(4) | 0.0587(2) | −0.0460(4) |
| O(41) | 0.9907(4) | 0.1512(2) | −0.1777(5) |
| O(12) | 0.2660(2) | 0.0702(2) | −0.3623(4) |
| O(22) | −0.0280(2) | −0.0183(2) | −0.1851(4) |
| C(11) | 0.7256(6) | 0.2439(3) | −0.1460(6) |
| C(21) | 0.5643(5) | 0.1999(2) | −0.0966(6) |
| C(31) | 0.6677(5) | 0.1268(2) | −0.0930(6) |
| C(41) | 0.8293(5) | 0.1676(2) | −0.1482(6) |
| C(12) | 0.1210(6) | 0.0325(3) | −0.4440(6) |
| C(22) | −0.0194(5) | −0.0103(2) | −0.3611(5) |
| H(11) | 0.041 | 0.184 | 0.250 |
| H(21) | 0.166 | 0.234 | 0.250 |
| H(12) | 0.416 | 0.082 | 0.457 |
| H(22) | 0.543 | 0.135 | 0.334 |

TABLE 3. Atomic positions for **1b**-Ce

| Atom | *x* | *y* | *z* |
|---|---|---|---|
| Ce | 0.00528(4) | 0.26655(3) | 0.04191(4) |
| $O_w(1)$ | −0.1468(6) | 0.3692(5) | 0.3521(6) |
| $O_w(2)$ | 0.2141(6) | 0.3284(6) | 0.3482(6) |
| $O_w(3)$ | 0.521(3) | 0.159(2) | 0.532(3) |
| O(11) | 0.5233(6) | 0.4242(6) | 0.2848(6) |
| O(21) | 0.1955(5) | 0.5024(4) | 0.0078(5) |
| O(12) | 0.2916(5) | 0.1717(4) | −0.0550(6) |
| O(22) | 0.2916(5) | −0.1656(4) | 0.0538(6) |
| O(13) | −0.0153(6) | 0.2551(4) | −0.3313(6) |
| O(23) | 0.0017(5) | −0.0445(4) | −0.1955(5) |
| C(11) | 0.5107(8) | 0.4649(7) | 0.1293(9) |
| C(21) | 0.3642(7) | 0.5005(6) | 0.0030(8) |
| C(12) | 0.4049(7) | 0.0763(7) | −0.0253(8) |
| C(22) | 0.4042(8) | −0.0728(6) | 0.0237(8) |
| C(13) | −0.0063(7) | 0.1156(6) | −0.4295(8) |
| C(23) | 0.0021(7) | −0.0262(6) | −0.3660(8) |
| H(11) | −0.293 | 0.389 | 0.375 |
| H(21) | −0.125 | 0.334 | 0.459 |
| H(12) | 0.332 | 0.359 | 0.332 |
| H(22) | 0.207 | 0.389 | 0.457 |

TABLE 4. Atomic positions for **1c**-Ce

| Atom | *x* | *y* | *z* |
|---|---|---|---|
| Ce(1) | 0.36363(2) | 0.32562(1) | 0.48215(2) |
| Ce(2) | 0.54115(2) | 0.17636(1) | 1.00261(2) |
| $O_w(1)$ | 0.8511(3) | 0.1788(2) | 0.9700(5) |
| $O_w(2)$ | 0.7555(3) | 0.2037(2) | 1.3574(4) |
| $O_w(3)$ | 0 | 0 | 0 |
| O | 0.3927(3) | 0.2264(2) | 0.2122(3) |
| O(11) | 0.1411(3) | 0.3642(2) | 0.2068(3) |
| O(21) | −0.2583(3) | 0.3668(2) | 0.1178(4) |
| O(31) | −0.1116(3) | 0.6215(2) | 0.3755(3) |
| O(41) | 0.2955(3) | 0.6281(2) | 0.4025(4) |
| O(12) | 0.4851(3) | 0.1689(2) | 0.6123(3) |
| O(22) | 0.5500(3) | −0.0126(2) | 0.8280(3) |
| O(13) | 0.4869(3) | 0.5249(2) | 0.6844(3) |
| O(23) | 0.4093(3) | 0.3183(2) | 0.8546(3) |
| O(14) | 0.1010(3) | 0.1632(2) | 0.4114(4) |
| O(24) | −0.2271(3) | −0.0591(2) | 0.2018(4) |
| C(11) | 0.0753(4) | 0.4409(2) | 0.2338(4) |
| C(21) | −0.1096(4) | 0.4402(2) | 0.1992(4) |
| C(31) | −0.0445(4) | 0.5559(2) | 0.3083(4) |
| C(41) | 0.1432(4) | 0.5564(2) | 0.3266(4) |
| C(12) | 0.4922(4) | 0.0772(2) | 0.5424(4) |
| C(22) | 0.5232(4) | −0.0099(2) | 0.6456(4) |
| C(13) | 0.4962(3) | 0.5159(2) | 0.8606(4) |
| C(23) | 0.4586(3) | 0.4176(2) | 0.9431(4) |
| C(14) | 0.0474(4) | 0.0738(2) | 0.4599(5) |
| C(24) | −0.1037(4) | −0.0274(2) | 0.3644(5) |
| H(11) | 0.943 | 0.250 | 1.041 |
| H(21) | 0.918 | 0.125 | 1.000 |
| H(12) | 0.750 | 0.269 | 1.457 |
| H(22) | 0.889 | 0.228 | 1.375 |

## Main Structural Features

The determination of the crystal structure first allowed us to know the formula of each compound.

**1a**-Ce: $[Ce(H_2O)_2]_2(C_4O_4)_3$
**1b**-Ce: $[Ce(H_2O)_2]_2(C_4O_4)_3 \cdot 1.5H_2O$
**1c**-Ce: $[Ce,Ce(H_2O)_2]_2(OH)_2(C_4O_4)_5 \cdot 0.6H_2O$

The number of water molecules coordinated to the cerium atom is markedly lower than in the starting compound, **1**-Ce.

**1c**-Ce departs from the other two compounds by the presence of an isolated oxygen atom, O,

TABLE 5. Selected interatomic distances (Å)[a] and bond angles (°) in $[Ce(H_2O)_2]_2(C_4O_4)_3$ (**1a**-Ce)

| | | | | | |
|---|---|---|---|---|---|
| Around Ce | | | | | |
| Ce–$O_w$(1) | 2.540(4) | Ce–O(31) | 2.701(3) | Ce–O(12) | 2.599(3) |
| Ce–$O_w$(2) | 2.513(3) | Ce–O(31)$^{i}$ | 2.501(3) | Ce–O(22) | 2.476(3) |
| Ce–O(21) | 2.538(1) | Ce–O(41)$^{iii}$ | 2.410(3) | Ce–O(22)$^{ii}$ | 2.769(3) |
| Bridges | | | | | |
| Ce–Ce$^{i}$ | 4.4060(3) | Ce–O(31)–Ce$^{i}$ | 115.7(1) | | |
| Ce–Ce$^{ii}$ | 4.5547(3) | Ce–O(22)–Ce$^{ii}$ | 120.5(1) | | |
| Squarate sq(1) | | | | | |
| O(11)–C(11) | 1.240(4) | O(11)–C(11)–C(21) | 137.6(4) | | |
| O(21)–C(21) | 1.267(5) | C(11)–C(21)–C(31) | 90.9(3) | | |
| O(31)–C(31) | 1.267(5) | O(11)–C(11)–C(41) | 133.5(4) | | |
| O(41)–C(41) | 1.242(5) | C(21)–C(31)–C(41) | 91.0(3) | | |
| C(11)–C(21) | 1.469(6) | O(21)–C(21)–C(31) | 128.8(4) | | |
| C(21)–C(31) | 1.439(6) | C(31)–C(41)–C(11) | 89.3(3) | | |
| C(31)–C(41) | 1.460(6) | O(21)–C(21)–C(11) | 140.1(4) | | |
| C(41)–C(11) | 1.490(6) | C(41)–C(11)–C(21) | 88.7(3) | | |
| | | O(31)–C(31)–C(41) | 140.4(4) | | |
| | | O(31)–C(31)–C(21) | 128.5(4) | | |
| | | O(41)–C(41)–C(31) | 138.2(4) | | |
| | | O(41)–C(41)–C(11) | 132.5(4) | | |
| Squarate sq(2) | | | | | |
| O(12)–C(12) | 1.256(5) | O(12)–C(12)–C(22) | 140.4(4) | | |
| O(22)–C(22) | 1.252(5) | C(12)–C(22)–C(22)$^{ii}$ | 90.7(3) | | |
| C(12)–C(22) | 1.463(5) | O(12)–C(12)–C(22)$^{ii}$ | 130.3(4) | | |
| C(12)–C(22)$^{ii}$ | 1.447(6) | C(22)–C(12)–C(22)$^{ii}$ | 89.3(3) | | |
| | | O(22)–C(22)–C(12) | 141.0(4) | | |
| | | O(22)–C(22)–C(12)$^{ii}$ | 128.3(3) | | |
| Hydrogen bonds and van der Waals contacts | | | | | |
| Interlayer | | | | | |
| $O_w$(1)–O(11)$^{iii}$ | 2.883(5) | $O_w$(1)–$H_w$(11)–O(11)$^{iii}$ | 171.0(3) | | |
| $O_w$(1)–O(21)$^{iv}$ | 2.834(5) | $O_w$(1)–$H_w$(11)–O(21)$^{iv}$ | 126.4(2) | | |
| $O_w$(2)–O(11)$^{iv}$ | 2.718(5) | $O_w$(2)–$H_w$(22)–O(11)$^{iv}$ | 146.8(2) | | |
| $O_w$(1)–$O_w$(2) | 2.853(5) | | | | |
| $O_w$(1)–O(41) | 2.896(5) | | | | |
| $O_w$(1)–O(22) | 2.822(5) | | | | |
| Intralayer | | | | | |
| $O_w$(2)–O(12)$^{v}$ | 2.841(5) | $O_w$(2)–$H_w$(12)–O(12)$^{v}$ | 168.1(2) | | |

[a]Code of equivalent positions: $^{i} = 1 - x, -y, -z$; $^{ii} = -x, -y, -z$; $^{iii} = x - 1, \frac{1}{2} - y, \frac{1}{2} + z$; $^{iv} = x, \frac{1}{2} - y, \frac{1}{2} + z$; $^{v} = x, y, z + 1$; $^{vi} = x, \frac{1}{2} - y, z - \frac{1}{2}$.

TABLE 6. Selected interatomic distances (Å)[a] and bond angles (°) in $[Ce(H_2O)_2]_2(C_4O_4)_3 \cdot 1.5H_2O$ (**1b**-Ce)

| | | | | | |
|---|---|---|---|---|---|
| Around Cerium | | | | | |
| Ce–$O_w$(1) | 2.504(4) | Ce–O(21)$^{i}$ | 2.643(4) | Ce–O(13) | 2.601(4) |
| Ce–$O_w$(2) | 2.526(4) | Ce–O(12) | 2.408(4) | Ce–O(23) | 2.843(3) |
| Ce–O(21) | 2.622(4) | Ce–O(22) | 2.408(4) | Ce–O(23)$^{ii}$ | 2.495(4) |
| Bridges | | | | | |
| Ce–Ce$^{i}$ | 4.3562(4) | Ce–O(21)–Ce$^{i}$ | 111.7(1) | | |
| Ce–Ce$^{ii}$ | 4.6372(4) | Ce–O(23)–Ce$^{ii}$ | 120.5(1) | | |
| Squarate sq(1) | | | | | |
| O(11)–C(11) | 1.239(8) | O(11)–C(11)–C(21) | 135.0(6) | | |
| O(21)–C(21) | 1.281(7) | O(11)–C(11)–C(21)$^{iii}$ | 135.3(5) | | |
| C(11)–C(21) | 1.462(8) | O(21)–C(21)–C(11) | 134.8(6) | | |

*(continued)*

TABLE 6. *(continued)*

| | | | |
|---|---|---|---|
| Squarate sq(1) | | | |
| C(11)–C(21)$^{iii}$ | 1.463(9) | O(21)–C(21)–C(11)$^{iii}$ | 134.9(5) |
| | | C(11)–C(21)–C(11)$^{iii}$ | 90.3(5) |
| | | C(21)–C(11)–C(21)$^{iii}$ | 89.7(3) |
| Squarate sq(2) | | | |
| O(12)–C(12) | 1.254(7) | O(12)–C(12)–C(22) | 136.5(5) |
| O(22)–C(22) | 1.255(7) | C(12)–C(22)–C(12)$^{iv}$ | 90.2(5) |
| C(12)–C(22) | 1.459(9) | O(12)–C(12)–C(22)$^{iv}$ | 133.7(6) |
| C(12)–C(22)$^{iv}$ | 1.447(8) | C(22)–C(12)–C(22)$^{iv}$ | 89.7(5) |
| | | O(22)–C(22)–C(12) | 137.4(5) |
| | | O(22)–C(22)–C(12)$^{iv}$ | 132.4(6) |
| Squarate sq(3) | | | |
| O(13)–C(13) | 1.261(5) | O(13)–C(13)–C(23) | 130.5(5) |
| O(23)–C(23) | 1.255(7) | C(13)–C(23)–C(13)$^{v}$ | 89.7(5) |
| C(13)–C(23) | 1.448(9) | O(13)–C(13)–C(23)$^{v}$ | 139.2(6) |
| C(13)–C(23)$^{v}$ | 1.458(7) | C(21)–C(13)–C(23)$^{v}$ | 90.3(4) |
| | | O(23)–C(23)–C(13) | 129.4(4) |
| | | O(23)–C(23)–C(13)$^{v}$ | 140.9(5) |
| Hydrogen bonds and van der Waals contacts | | | |
| $O_w$(1)–O(11)$^{vi}$ | 2.583(6) | $O_w$(1)–$H_w$(11)–O(11)$^{vi}$ | 146.5(3) |
| $O_w$(1)–O(13)$^{vii}$ | 2.808(6) | $O_w$(1)–$H_w$(21)–O(13)$^{vii}$ | 165.0(3) |
| $O_w$(2)–O(11) | 2.601(6) | $O_w$(2)–$H_w$(12)–O(11) | 172.8(2) |
| $O_w$(2)–O(12) | 2.925(6) | | |
| $O_w$(2)–O(23)$^{ii}$ | 2.930(6) | | |
| O(12)–O(23) | 2.869(5) | | |

[a]Code of equivalent positions: $^{i} = -x, 1-y, -z$; $^{ii} = -x, -y, -z$; $^{iii} = 1-x, 1-y, -z$; $^{iv} = 1-x, -y, -z$; $^{v} = -x, -y, -z-1$; $^{vi} = x-1, y, z$; $^{vii} = x, y, 1+z$.

TABLE 7. Selected interatomic distances (Å)[a] and bond angles (°) in $[Ce{\cdot}Ce(H_2O)_2]_2(OH)_2(C_4O_4)_5 \cdot 0.65H_2O$ (1c-Ce)

| | | | |
|---|---|---|---|
| Around cerium | | | |
| Ce(1)–O | 2.278(2) | Ce(2)–O$^{iii}$ | 2.280(2) |
| Ce(1)–O(11) | 2.489(2) | Ce(2)–O(21)$^{iv}$ | 2.456(2) |
| Ce(1)–O(31)$^{i}$ | 2.701(3) | Ce(2)–O(12) | 2.674(2) |
| Ce(1)–O(41)$^{ii}$ | 2.527(2) | Ce(2)–O(22)$^{i}$ | 2.641(2) |
| Ce(1)–O(12) | 2.653(2) | Ce(2)–O(22)$^{v}$ | 2.596(2) |
| Ce(1)–O(13) | 2.588(2) | Ce(2)–O(23) | 2.569(2) |
| Ce(1)–O(13)$^{ii}$ | 2.576(2) | Ce(2)–O(24)$^{vi}$ | 2.504(2) |
| Ce(1)–O(23) | 2.590(2) | Ce(2)–$O_w$(1) | 2.562(3) |
| Ce(1)–O(14) | 2.434(2) | Ce(2)–$O_w$(2) | 2.575(2) |
| Bridges | | | |
| Ce(1)–Ce(2)$^{viii}$ | 4.4532(2) | Ce(1)–O–Ce(2)$^{viii}$ | 117.05(8) |
| Ce(1)–Ce(1)$^{ii}$ | 4.4039(2) | Ce(1)–O(13)–Ce(1)$^{ii}$ | 117.05(8) |
| Ce(2)–Ce(2)$^{v}$ | 4.4407(2) | Ce(2)–O(12)–Ce(2)$^{v}$ | 116.00(9) |
| Ce(1)–Ce(2) | 4.4679(2) | Ce(1)–O(12)–Ce(2) | 114.03(8) |
| | | Ce(1)–O(23)–Ce(2) | 120.00(9) |
| Squarate sq(1) | | | |
| O(11)–C(11) | 1.268(4) | O(11)–C(11)–C(21) | 131.4(2) |
| O(21)–C(21) | 1.248(4) | O(11)–C(11)–C(41) | 137.1(2) |
| O(31)–C(31) | 1.240(4) | O(21)–C(21)–C(11) | 132.4(3) |
| O(41)–C(41) | 1.254(3) | O(21)–C(21)–C(31) | 137.3(3) |
| C(11)–C(21) | 1.444(4) | O(31)–C(31)–C(21) | 136.9(3) |
| C(21)–C(31) | 1.486(4) | O(31)–C(31)–C(41) | 134.6(2) |
| C(31)–C(41) | 1.483(4) | O(41)–C(41)–C(11) | 136.5(3) |

*(continued)*

TABLE 7. *(continued)*

| | | | |
|---|---|---|---|
| Squarate sq(1) | | | |
| C(41)–C(11) | 1.451(4) | O(41)–C(41)–C(31) | 133.3(3) |
| | | C(21)–C(11)–C(41) | 91.1(3) |
| | | C(11)–C(21)–C(31) | 90.3(2) |
| | | C(21)–C(31)–C(41) | 88.2(2) |
| | | C(31)–C(41)–C(11) | 90.1(3) |
| Squarate sq(2) | | | |
| O(12)–C(12) | 1.257(4) | O(12)–C(12)–C(22) | 129.1(3) |
| O(22)–C(22) | 1.263(4) | O(12)–C(12)–C(22)$^{ix}$ | 141.1(3) |
| C(12)–C(22) | 1.463(4) | O(22)–C(22)–C(12) | 129.2(3) |
| C(12)–C(22)$^{ix}$ | 1.460(4) | O(22)–C(22)–C(12)$^{ix}$ | 140.7(3) |
| | | C(22)–C(12)–C(22)$^{ix}$ | 89.8(2) |
| | | C(12)–C(22)–C(12)$^{ix}$ | 90.2(2) |
| Squarate sq(3) | | | |
| O(13)–C(13) | 1.256(4) | O(13)–C(13)–C(23) | 129.6(2) |
| O(23)–C(23) | 1.268(3) | O(13)–C(13)–C(23)$^{x}$ | 140.7(3) |
| C(13)–C(23) | 1.459(4) | O(23)–C(23)–C(13) | 128.8(3) |
| C(13)–C(23)$^{x}$ | 1.447(4) | O(23)–C(23)–C(13)$^{x}$ | 140.9(3) |
| | | C(23)–C(13)–C(23)$^{x}$ | 89.7(2) |
| | | C(13)–C(23)–C(13)$^{x}$ | 90.3(2) |
| Squarate sq(4) | | | |
| O(14)–C(14) | 1.246(4) | O(14)–C(14)–C(24) | 134.0(3) |
| O(24)–C(24) | 1.246(4) | O(14)–C(14)–C(24)$^{vi}$ | 135.5(2) |
| C(14)–C(24) | 1.465(3) | O(24)–C(24)–C(14) | 134.4(3) |
| C(14)–C(24)$^{vi}$ | 1.471(5) | O(24)–C(24)–C(14)$^{vi}$ | 136.0(3) |
| | | C(24)–C(14)–C(24)$^{vi}$ | 90.4(2) |
| | | C(14)–C(24)–C(14)$^{vi}$ | 89.6(2) |
| Hydrogen bonds and van der Waals contacts | | | |
| O(11)–O(13)$^{ii}$ | 2.796(3) | | |
| O(11)–$O_w$(1)$^{vii}$ | 2.823(3) | O(11)–$H_w$(11)$^{vii}$–$O_w$(1)$^{vii}$ | 167.1(2) |
| O(21)–O(23)$^{vii}$ | 2.692(3) | | |
| O(21)–$O_w$(2)$^{vii}$ | 2.882(4) | | |
| O(31)–O(23)$^{i}$ | 2.887(3) | | |
| O(31)–$O_w$(2)$^{x}$ | 3.087(3) | O(31)–$H_w$(22)$^{x}$–$O_w$(2)$^{x}$ | 125.5(2) |
| O(41)–$O_w$(2) | 2.794(4) | O(41)–$H_w$(12)$^{x}$–$O_w$(2)$^{x}$ | 170.7(1) |
| O(12)–O(23) | 2.737(3) | | |
| O(12)–O(24)$^{vi}$ | 2.894(4) | | |
| O(22)–O(22)$^{v}$ | 2.775(3) | | |
| O(22)–$O_w$(1) | 2.810(3) | | |
| O(22)–$O_w$(2)$^{v}$ | 2.850(3) | | |
| O(13)–O(13)$^{ii}$ | 2.696(3) | | |
| O(14)–$O_w$(2)$^{vii}$ | 2.913(4) | O(14)–$H_w$(22)$^{vii}$–$O_w$(2)$^{vii}$ | 138.9(2) |
| O(24)–$O_w$(3) | 2.620(3) | | |
| O(24)–$O_w$(3)$^{xi}$ | 2.620(3) | | |
| $O_w$(1)–$O_w$(3)$^{iv}$ | 2.899(3) | $O_w$(3)–$H_w$(21)$^{iv}$–$O_w$(1)$^{iv}$ | 166.0(1) |

[a]Code of equivalent positions: $^{i} = -x, 1-y, 1-z$; $^{ii} = 1-x, 1-y, 1-z$; $^{iii} = x, y, 1+z$; $^{iv} = 1+x, y, 1+z$; $^{v} = 1-x, -y, 2-z$; $^{vi} = -x, -y, 1-z$; $^{vii} = x-1, y, z-1$; $^{viii} = x, y, z-1$; $^{ix} = 1-x, -y, 1-z$; $^{x} = 1-x, 1-y, 2-z$; $^{xi} = -x, -y, -z$.

that was considered as pertaining to a hydroxide ion rather than to an oxide ion, though no H atom could be located. The presence of $O^{2-}$ would imply a mixed Ce(III)–Ce(IV) compound and consequently two types of cerium environment differing in cerium–oxygen bond lengths and number which is not the case (Table 7). Moreover, the crystals are white and not yellow as would be a Ce(IV) containing compound.

The major features of these compounds compared to those prepared in an open system are the diversity and in some cases the novelty of the modes of coordination of the squarate ligand. In the three compounds some of the ligands are mono- and/or

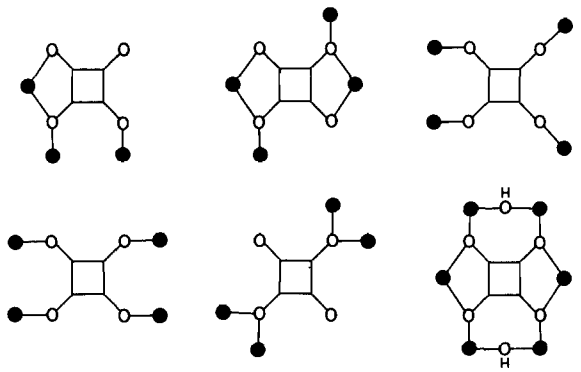

Fig. 1. Schematization of the different modes of coordination of the squarate anion in **1a**-Ce, **1b**-Ce and **1c**-Ce.

bis-chelating; these or other ligands create Ce–O–Ce bridges. In **1c**-Ce, hydroxo Ce–OH–Ce bridges are also present. Even the fourfold monodentate mode of coordination that is the oldest one known for the squarate ligand [12] gives rise here to an original arrangement of metal atoms. The set of the observed modes is schematically presented in Fig. 1. The number of Ce atoms related by a squarate ligand is high: in most cases it is equal to 4; twice in **1c**-Ce it reaches the value of 6 and is only once equal to 3 in **1a**-Ce. Correlatively, squarate oxygen atoms widely predominate in the close environment of the cerium atoms. Through the Ce–O–Ce bridges they build up a dense framework which is bidimensional in **1a**-Ce and tridimensional in **1b**-Ce and **1c**-Ce.

*The Ce–O–Ce Bridges*

In the three compounds, the cerium atoms are ninefold coordinated. In **1c**-Ce there are two symmetrically independent cerium atoms, namely Ce(1) and Ce(2): it is noticeable that Ce(1) is not bound to any water molecule but to eight squarate oxygen atoms and one hydroxyl group. Ce(2) is bound to the same hydroxyl plus two water molecules and six squarate oxygen atoms.

The Ce–OH distances are by far the shortest cerium–oxygen distances. They are equal: Ce(1)–O = 2.278(2), Ce(2)–O = 2.280(2) Å. Thus the hydroxy bridge Ce(1)–OH–Ce(2) is quite symmetrical. It is a single bridge with an angle of 156.0(1)°.

The other cerium–oxygen distances range from 2.408(4) to 2.843(3) Å, with the same mean value in each compound: 2.56 Å in **1a**-Ce and **1b**-Ce and 2.57 Å in **1c**-Ce. Many of the squarato oxygen atoms are engaged in double Ce–O–Ce bridges. Some of them are strictly centrosymmetric.

In **1a**-Ce and **1b**-Ce, the chelating ligands bite asymmetrically since each of them has one oxygen atom bound to two cerium atoms (Fig. 1) and the other one to one cerium atom. Accordingly, large differences arise between the bridging Ce–O distances.

**1a**-Ce O(31)–Ce = 2.501(3) and O(31)–Ce = 2.701(3) Å
O(22)–Ce = 2.476(3) and O(22)–Ce = 2.769(3) Å
**1b**-Ce O(23)–Ce = 2.843(3) and O(23)–Ce = 2.495(3) Å

There is no other bridge in **1a**-Ce. In **1b**-Ce there is a second kind of double bridge which is more symmetric.

**1b**-Ce O(21)–Ce = 2.622(4) and O(21)–Ce = 2.643(4) Å

The corresponding squarate ligand is not chelating but involves instead two oxygen atoms *trans* to each other (see below).

In **1c**-Ce, the doubly bridging oxygen atoms pertain to bis-chelating ligands. Each of them is bound to two cerium atoms which is only partly the case in **1a**-Ce and **1b**-Ce. Therefore the discrepancies in Ce–O distances are far less pronounced than previously:

**1c**-Ce O(12)–Ce(1) = 2.653(2) and O(12)–Ce(2) = 2.674(2) Å
O(22)–Ce(2) = 2.641(2) and O(22)–Ce(2) = 2.595(2) Å
O(13)–Ce(1) = 2.576(2) and O(13)–Ce(1) = 2.588(2) Å
O(23)–Ce(1) = 2.590(2) and O(23)–Ce(2) = 2.569(2) Å

Separations between nearest Ce atoms have their maximal and minimal values in **1b**-Ce: 4.6372(4) and 4.3562(4) Å. Two closer values are found in **1a**-Ce: 4.5554(4) and 4.4060(3) Å. In **1c**-Ce, the gap is even lower: 4.4679(2), 4.4407(2), 4.4039(2) Å in the double bridges and 4.4582(2) Å in the single bridges.

The basic frame of **1a**-Ce and **1b**-Ce is made of unlimited chains of doubly bridged cerium atoms. In **1a**-Ce, the chains zigzag along the *a* axis about the planes $z = 0$ and $z = \frac{1}{2}$ from which the cerium atoms do not deviate by more than 0.05 Å. The chain repeat unit is made of two non-equivalent double bridges whose respective mean planes and Ce···Ce axes are almost perpendicular (Fig. 2(a)). In **1b**-Ce, there are also alternating non-equivalent double bridges, but the chains are linear with the cerium atom standing about 0.3 Å from the *b* axis. Again, the mean planes of two successive bridges are nearly perpendicular (Fig. 2(b)).

In **1c**-Ce, a bidimensional framework results from the side interconnection of the chains of doubly bridged cerium atoms by the single hydroxy bridges. The cerium atoms form puckered nets around the planes $x = \frac{1}{2}$. It is noteworthy that they gather into pseudo hexagonal cycles in which two opposite sides are single bridges and the four other sides are double bridges. Every side is shared by two cycles. There are two crystallographically independent cycles per unit cell. Equivalent cycles repeat by the translation c so as to form two types of ribbons which alternate along the *b* axis (Fig. 3).

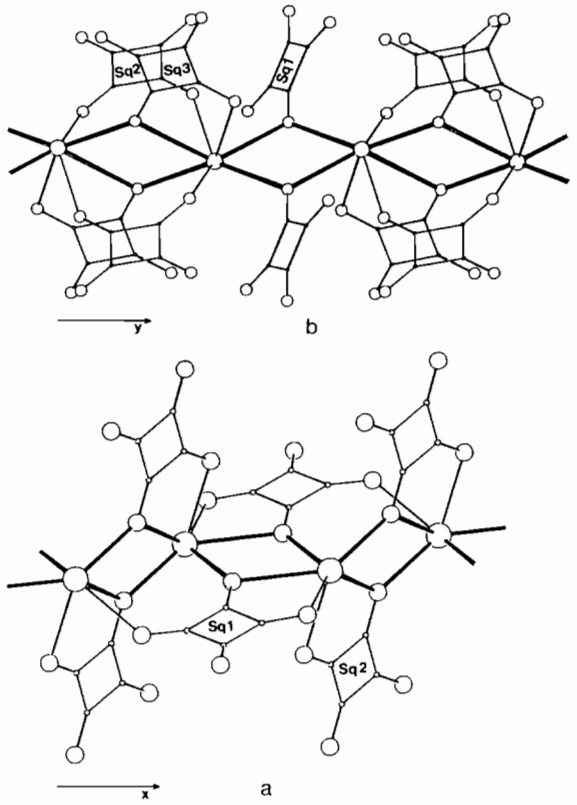


Fig. 2. View of a chain of double bridges in: (a) **1a**-Ce and (b) **1b**-Ce.

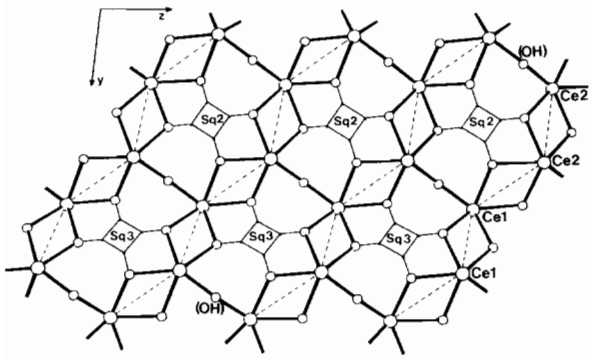


Fig. 3. View of a layer of single and double bridges in **1c**-Ce.

*The Squarate Ligands*

There are two crystallographically independent squarate ligands in **1a**-Ce, three in **1b**-Ce and four in **1c**-Ce. The different modes of coordination they show are new with respect to what was observed so far in transition metal squarates from X-ray single crystal studies [2]. Some of these modes were recently observed in alkali-earth squarates [5–8], particularly chelation that is observed in the three present compounds.

A transition metal being chelated by the squarate anion was postulated several times on the fragile basis of spectroscopic data [3]. In some papers, chelation seems to go without saying and the spectroscopic data are interpreted on the basis of this *a priori* statement. This probably comes from a misleading analogy with the oxalate anion. Actually the squarate geometry and the usually measured metal–oxygen bond lengths are such that the chelation can only be achieved through a wide deformation of the involved O–C–C angles. On bite angle considerations, M. Julve *et al.* established that only the largest cations have a chance to be chelated [13]. It appears that it is the case for the lanthanides +3, as for the alkali-earth cations [5–8]. The effect of chelation on the O–C–C angles is well marked: these angles range from 128 to 131° inside the chelate and conversely from 139 to 141° outside, against 133 to 135° for usual non-chelating squarate anions.

Among the various squarate ligands encountered in this study, some are strictly centrosymmetric and a few have one or two non-metal-bound oxygen atoms.

The ligand sq(1) in **1b**-Ce is centrosymmetric with two metal-free and two metal-bridging oxygen atoms so that it relates four cerium atoms (Fig. 4). Consequently, the two couples of C–O bonds differ by 0.04 Å. There is no significant deviation from planarity and the carbon cycle is a square.

The ligand sq(1) in **1a**-Ce has one metal-free oxygen atom, O(11). It is chelating through the atoms O(21) and O(31) and monodentate at O(41) (Fig. 5). Even if the bite Ce–O bond lengths of 2.538(3) and 2.701(3) Å are markedly different, the chelation can be retained on comparing the adjacent O–C–C angles which show gaps of 11–12° on the side of the chelate and only 4–5° on the opposite side. Also consistent with the one-sided chelation is the slight trapezoid deformation of the C-cycle with the bite C–C bond 0.05 Å shorter (1.439(6) Å) than the opposite one (1.490(6) Å) and the lateral lengths being intermediate (1.460(6)

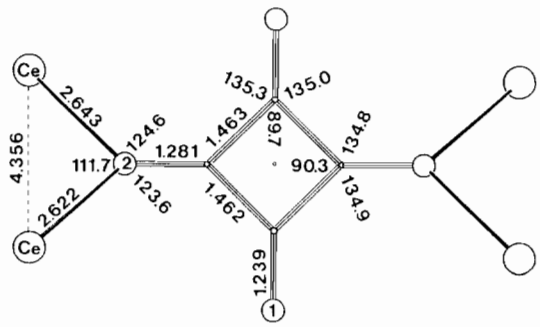


Fig. 4. The coordination mode of the squarate anion sq(1) in **1b**-Ce.

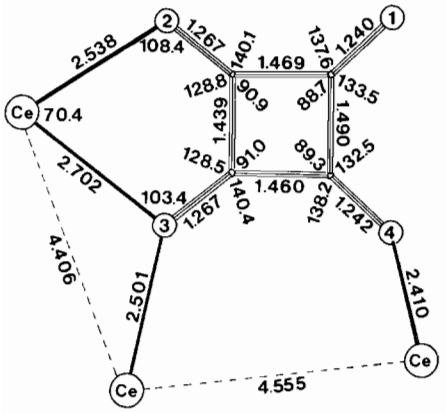


Fig. 5. The coordination mode of the squarate anion sq(1) in **1a**-Ce.

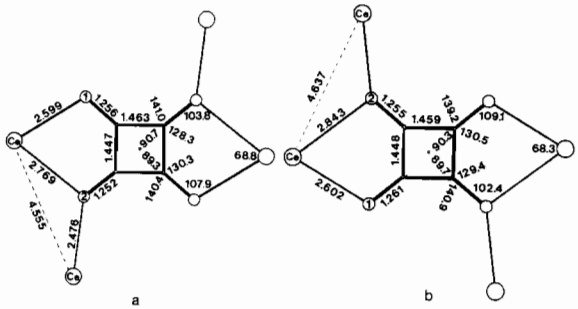


Fig. 6. The coordination mode of the squarate anions (a) sq(2) in **1a**-Ce and (b) sq(3) in **1b**-Ce.

and 1.469(6) Å). The cycle is quasi planar. However this is not a case of pure chelation since one of the biting oxygen atoms, namely O(31), is also bound to another cerium atom related to the chelated one by centrosymmetry and closer to O(31) by 0.2 Å. A similar mode of coordination was found by Robl and Weiss in the strontium squarate trihydrate of type I [6]. Since the cation is less charged, the deformation of the ligand is less pronounced: gaps of 7–8° in the pairs of the O–C–C angles and a dispersion limited to 0.02 Å in the C–C bonds.

Four squarate ligands are bis-chelating: they are sq(2) in **1a**-Ce (Fig. 6(a)), Sq(3) in **1b**-Ce (Fig. 6(b)) and sq(2) and sq(3) in **1c**-Ce (Fig. 7). All are centrosymmetric and do not depart from planarity. The gaps within adjacent pairs of O–C–C angles range from 9 to 13°. The C-cycles are either slightly rectangular or quasi square, and the C–O bond lengths range within a short if significant interval: 1.252(5) to 1.268(4) Å.

In **1a**-Ce and **1b**-Ce (Fig. 6), one oxygen atom of either bite is also bound to another cerium atom which is centrosymmetrically related to the chelated one as was previously the case for the mono-chelating ligand. Here again, the Ce–O bonds without the chelates are the shortest ones: 2.476(3) Å in **1a**-Ce and 2.495(3) Å in **1b**-Ce, and the Ce–O bonds within the chelates show marked differences: 2.599(3) versus 2.769(3) Å in **1a**-Ce and 2.602(4) versus 2.843(3) Å in **1b**-Ce. Such a situation was observed by Robl *et al.* in the strontium squarate trihydrate of type II [7]. The above remark about the ligand less deformed than in the present compounds is still valid here.

The situation is quite different in **1c**-Ce (Fig. 7) where each oxygen atom is bound to two cerium atoms, one chelated, the other not. The non-chelated

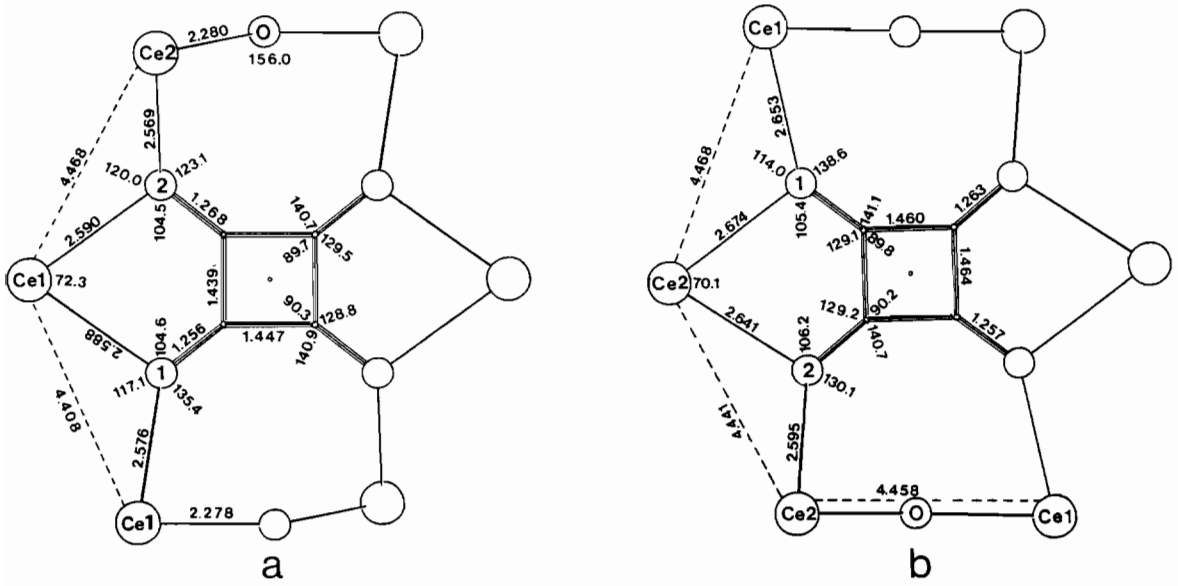


Fig. 7. The coordination mode of the squarate anions (a) sq(2) and (b) sq(3) in **1c**-Ce.

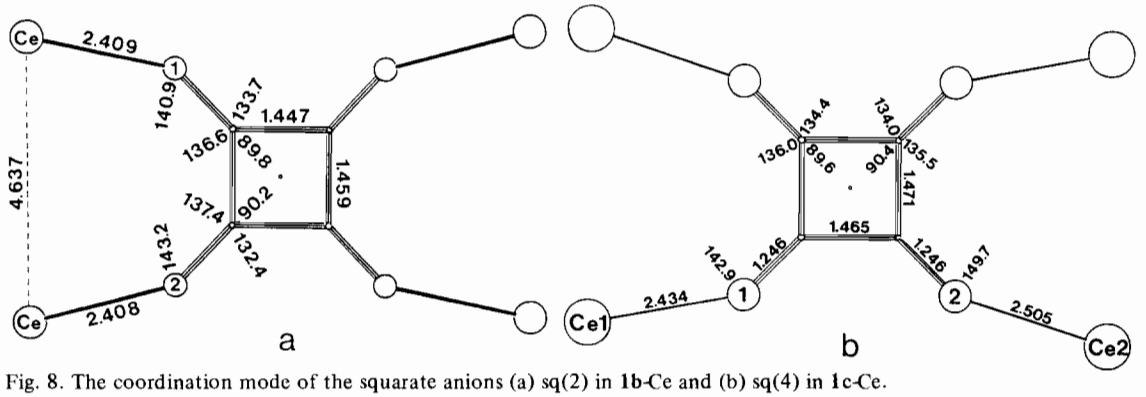


Fig. 8. The coordination mode of the squarate anions (a) sq(2) in **1b**-Ce and (b) sq(4) in **1c**-Ce.

cerium atoms are related two by two by the hydroxy bridges. The Ce–O bond lengths are much less dispersed and the chelation is more symmetric than previously: 2.641(2) and 2.674(2) Å in sq(2); 2.588(2) and 2.590(2) Å in sq(3). This is a fairly new situation.

Three squarate ligands are tetrakis-monodentate: they are sq(2) in **1b**-Ce, sq(1) and sq(4) in **1c**-Ce. However, the atom arrangements do not have the pseudo fourfold symmetry observed in the rare known cases of a tetrakis-monodentate squarate anion [12, 14].

Sq(2) in **1b**-Ce (Fig. 8(a)) and sq(4) in **1c**-Ce (Fig. 8(b)) are centrosymmetrical and planar with quasi-square C-cycles. There are no significant differences within C–C and within C–O bond lengths, and O–C–C angles do not depart by more than 2.5° from the ideal value of 135°. The cerium atoms they relate adopt a binary symmetry arrangement due to the double bridges which paired them.

Sq(1) in **1c**-Ce (Fig. 9) has no imposed symmetry. The arrangement of the cerium atoms bound to it comes from the fact that only two of the cerium atoms are related by the same bridge.

*Description of the Crystal Structures*

It is convenient to describe the crystal structures from the basic arrays of Ce–O–Ce bridges described above: unlimited chains in **1a**-Ce and **1b**-Ce and bidimensionally extended collateral cycles in **1c**-Ce. These arrangements are diversely related so as to generate bi- or tridimensional structures.

In **1a**-Ce, the chains are interconnected by the bis-chelating sq(2) ligands into layers perpendicular to the *b* axis (Fig. 10). Interlayer H bonds and van der Waals interactions strengthen the structure (Table 5).

**1b**-Ce has a tunnel structure resulting from a double system of connection of the chains by the ligands sq(1) and sq(2) in the (001) planes and sq(3) in the (100) planes. The tunnels are parallel to the *b* axis and their walls are covered with the ligands (Fig. 11): sq(3) makes an angle of 2.9(2)°

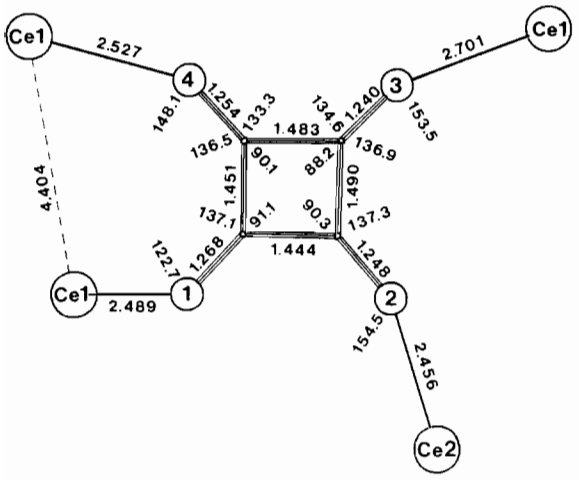


Fig. 9. The coordination mode of the squarate anion sq(1) in **1c**-Ce.

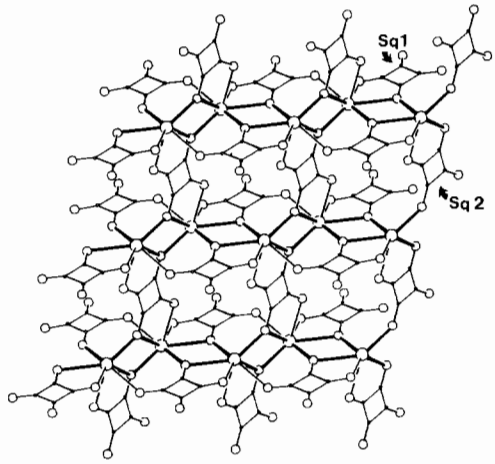


Fig. 10. View of a layer in the structure of **1a**-Ce: chains like that of Fig. 2(a) are interconnected by the squarate anions sq(2).

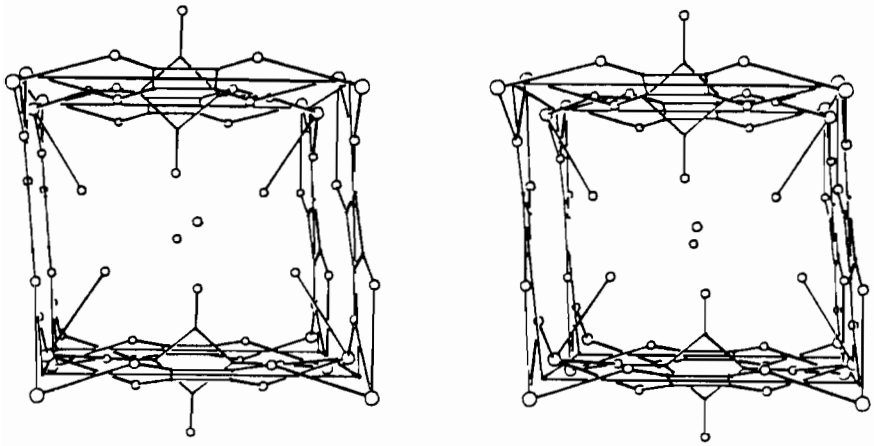

Fig. 11. Stereoscopic view down the *b* axis of the unit cell of **1**b-Ce showing the tunnel structure: chains like that of Fig. 2(b) are interconnected by the squarate anions sq(1) and sq(2) on one wall and sq(3) on the other one.

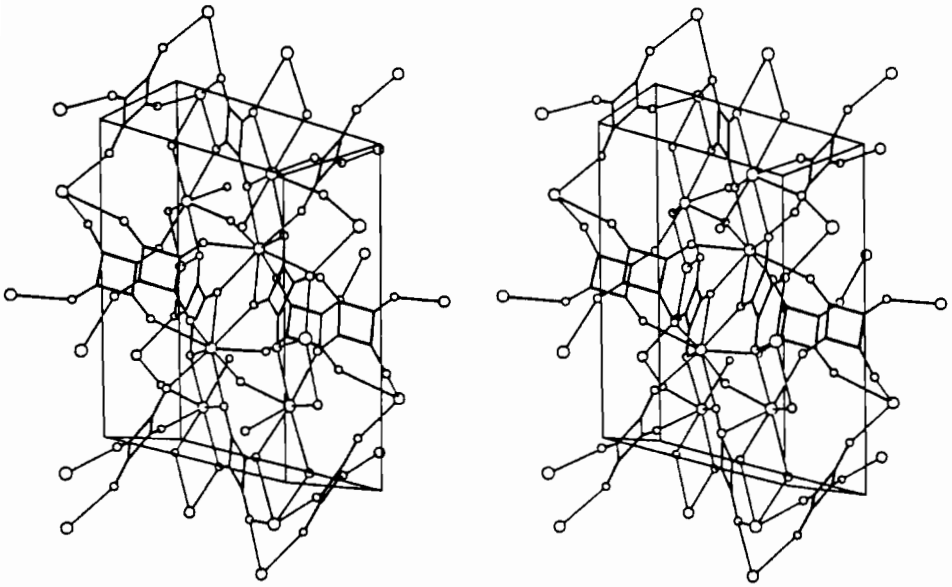

Fig. 12. Stereoscopic view of the unit cell of **1**c-Ce: layers like that of Fig. 3 are interconnected by the squarate anions sq(1) and sq(4).

with the (100) plane; sq(2) makes an angle of 9.9(1)° with the (001) plane while sq(1) is much more tilted away with an angle of 58.2(1)° with the same plane. The sq(1) free oxygen atoms and the water molecules coordinated to the cerium atoms stand out of the walls thus reducing the size of the tunnel. There remains space enough to accommodate two water molecules per unit cell. Their oxygen atoms stand at no less than 3.15 Å from the closest oxygen atoms. This explains why they were found with an occupancy of 75% and a rather high thermal motion coefficient. This structure compares with that of $Ca(C_4O_4)\cdot 2.5H_2O$ that was studied by Robl *et al.* who compared it with a zeolite [8].

**1**c-Ce has a tridimensional structure which results from the connection of the layers described above by the tetrakis-monodentate ligands, sq(1) and sq(4) (Fig. 12). The alternating inversions through centres at $(0, \frac{1}{2}, 0)$ and $(0, \frac{1}{2}, \frac{1}{2})$ give rise to stacking sq(1) ligands. The distances between the C-square mean planes are alternately 3.60 and 3.17 Å to which correspond overlapping extents of nearly 25% and 20%, respectively (Fig. 13). Therefore the stacks are strongly dimerized [15]. Other van der Waals interactions and H bonds are gathered in Table 7. Non-stoichiometric intervening water molecules are distributed around the cell vertices which are the farthest points from any squarate ligand.

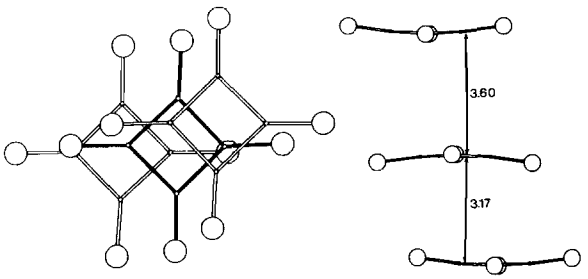


Fig. 13. Neighbouring overlapping sq(1) ligands in 1c-Ce.

It is noteworthy that chelation and bridge formation resulting from dehydration increase dramatically the density with respect to 1-Ce: $\rho = 2.28$ (1-Ce), 2.55 (1b-Ce), 2.75 (1a-Ce), 3.01 (1c-Ce) g/cm$^3$.

## Extension to the Other Lanthanides

The conditions of preparation of the three compounds, with extension to the other lanthanides have been and still are being investigated. If the ease of dehydration of 1-Ce (TDA peak at 130 °C [1]) was one major feature governing its transformation into 1a-Ce in the conditions described in 'Experimental', then similar results were to be expected from the other 1-Ln compounds under similar conditions, since they show one or two TDA dehydration peaks around 130 °C: 1-La at 130 °C, 1-Pr at 105 and 146 °C, 1-Nd at 102 and 141 °C [1]. As a matter of fact, it was possible to transform all the 1-Ln compounds into 1a-Ln by heating them in water inside a closed vessel. Temperature and duration are not as critical parameters as could be expected from reading the 'Experimental'. Indeed the transformation can be achieved at temperatures as low as 90 °C, but the use of higher temperatures is time saving since the transformation was observed to be over in one day by operating at 135 °C. At 150 °C, pure 1a-Ln compounds are still produced. However, it appeared that the ease of dehydration was not the main feature governing the transformation since it was possible to transform 2-Sm, which is the first member of the 2-Ln family, into 1a-Sm despite a dehydration TDA peak at 172 °C [1]. The transformation was total at 150 °C. It could not be achieved for the following members of the 2-Ln family, even upon heating upto 200 °C.

Another pseudo-hydrothermal route was successfully used that consisted in reacting lanthanide sesquioxide with a slight excess of squaric acid in water at *c.* 150 °C in a closed steel container. The 1a-Ln family then could be extended to Eu which corresponds to the second member of the 2-Ln family [1]. For Ce and Pr, the $CeO_2$ and $Pr_6O_{11}$ oxides were used. Oxidation of squaric acid by Ln(IV) takes place as a side reaction that yields oxidation by-products, probably oxalates and oxalatosquarates as was observed in previous experiments [16].

The unit-cell constants of compounds 1a-La to 1a-Eu were calculated from X-ray powder diagrams by least-squares refinements of fourteen reflections (Cu K$\alpha$ radiation). They are listed in Table 8. Unit-cell constants and volumes decrease from La to Sm. However, they increase from Sm to Eu. This could come from the fact that the Eu phase obtained was not pure.

Up to now, 1b-Ce could not be produced again. It is most likely that the thermal story of the compound 1b-Ce described above was not as simple as reported in 'Experimental' for some unknown reason that we keep on attempting to elucidate. In view of the quantity obtained, 1c-Ce was produced as a minor product under the conditions of the above see 'Experimental'. Experiments to get it as a pure product, or at least to improve its yield, are currently being developed.

## Thermal Behaviour of the 1a-Ln Compounds

1a-La, 1a-Ce, 1a-Pr, 1a-Nd and 1a-Sm were submitted to TGA and TDA analyses, while 1a-Eu was not since it could not be obtained as a pure phase. The experimental conditions were described in ref. 1. As for the 1-Ln compounds [1], total dehydration was observed before squarate decomposition, except for 1a-Ce. Dehydration of 1a-La, 1a-Pr, 1a-Nd and

TABLE 8. Unit-cell constants for the 1a-Ln compounds

| | 1a-La | 1a-Ce | 1a-Pr | 1a-Nd | 1a-Sm | 1a-Eu |
|---|---|---|---|---|---|---|
| $a$ (Å) | 7.20(1) | 7.143(2) | 7.10(1) | 7.06(2) | 7.00(2) | 7.06(2) |
| $b$ (Å) | 17.00(2) | 16.940(2) | 16.84(3) | 16.72(3) | 16.58(4) | 16.71(4) |
| $c$ (Å) | 7.02(1) | 6.994(1) | 6.96(1) | 6.91(1) | 6.84(2) | 6.89(2) |
| $\beta$ (°) | 101.4(2) | 101.24(2) | 101.7(2) | 101.6(2) | 101.7(3) | 102.0(3) |
| $V$ (Å$^3$) | 842(5) | 830.0(4) | 815(5) | 800(6) | 777(6) | 796(7) |

**1a**-Sm occurs in two steps. The corresponding TDA endothermic peaks are at *c.* 240 and 305 °C, about 100 to 150 °C higher than for the **1**-Ln compounds. This is consistent with the lower water coordination of two molecules per lanthanide. In the TGA curves of **1a**-La, **1a**-Pr and **1a**-Nd, the first step corresponds to the departure of *c.* 75% of the water and the second to the remaining 25%. This implies the intermediary formation of a compound having about 0.5 water molecule per lanthanide. In **1a**-Sm, the first dehydration step corresponds to the departure of *c.* 85% of the water content, and the second step to the remaining 15%. Decomposition of the anhydrous **1a**-La, **1a**-Pr and **1a**-Nd squarates starts short after dehydration is over, at around 360 °C, i.e. 50 to 70 °C lower than for the **1**-Ln compounds while that of **1a**-Sm starts at the same temperature as that of **2**-Sm. The decomposition process results in the formation of the relevant oxides. It is marked by a main TDA exothermic peak having its maximum at nearly the same temperature as for the corresponding **1**-Ln or **2**-Sm compound. However, differences in extra peaks and shoulders with respect to the latter were observed, suggesting that the amorphous phases resulting from the dehydration of a **1**-Ln and a **1a**-Ln compound present some structural discrepancies. Large angle X-ray scattering (LAXS) experiments are planned to check this point.

**1a**-Ce presents only one dehydration TDA peak at 238 °C, again corresponding to the departure of *c.* 75% of the water content. The TGA analysis shows that the second dehydration step is included into the squarate decomposition step. The dehydration–decomposition process starts at *c.* 260 °C, i.e. 40 °C lower than for **1**-Ce, and is very exothermic. It takes place over a temperature range slightly larger than the decomposition of the anhydrous **1**-Ce. The maximum of the TDA peak is at 305 °C, and the resulting oxide is the cerium(IV) oxide $CeO_2$.

## Acknowledgements

Financial support from Rhône Poulenc, Division Minérale Fine, and C.N.R.S. is gratefully acknowledged.

## References

1 J.-F. Petit, A. Gleizes and J.-C. Trombe, *Inorg. Chim. Acta, 167* (1990) 000.
2 J.-C. Trombe, J.-F. Petit and A. Gleizes, *New J. Chem., 12* (1988) 197, and refs. therein.
3 R. West and H. Y. Niu, *J. Am. Chem. Soc., 85* (1963) 2589; S. M. Condren and H. O. McDonald, *Inorg. Chem., 12* (1973) 57; J. T. Wrobleski and D. B. Brown, *Inorg. Chem., 17* (1978) 2959; H. Toftlund, *J. Chem. Soc., Chem. Commun.*, (1979) 837.
4 E. Riegler, *Dissertation,* München University (1979); A. Weiss, E. Riegler, I. Alt and C. Robl, *Z. Naturforsch., Teil B, 41* (1986) 18; C. Robl and A. Weiss, *Z. Naturforsch., Teil B, 41* (1986) 1341.
5 C. Robl and A. Weiss, *Z. Naturforsch., Teil B, 41* (1986) 1485.
6 C. Robl and A. Weiss, *Z. Naturforsch., Teil B, 41* (1986) 1490.
7 C. Robl, V. Gnutzmann and A. Weiss, *Z. Anorg. Allg. Chem., 549* (1987) 187.
8 C. Robl and A. Weiss, *Mater. Res. Bull., 22* (1987) 373.
9 *SDP Structure Determination Package,* Enraf-Nonius, Delft, 1979; C. K. Johnson, *ORTEP,* a Fortran thermal ellipsoid plot program for crystal structure illustrations, *Report ORNL-3794,* Oak-Ridge National Laboratory, TN, 1965.
10 *International Tables for X-ray Crystallography,* Vol. 4, Kynoch Press, Birmingham, 1974, Tables 2.2A and 2.3.1.
11 A. Mosset, J. J. Bonnet and J. Galy, *Acta Crystallogr., Sect. B, 33* (1977) 2633.
12 M. Habenschuss and B. C. Gerstein, *J. Chem. Phys., 61* (1974) 852.
13 X. Solans, M. Aguilo, A. Gleizes, J. Faus and M. Julve, *Inorg. Chem.*, (1990) in press.
14 J.-C. Trombe and A. Gleizes, *C.R. Acad. Sci. Paris, II-302* (1986) 21.
15 W. M. Macintyre and M. S. Werkema, *J. Chem. Phys., 42* (1964) 3563.
16 J.-C. Trombe, J.-F. Petit and A. Gleizes, *Lanthanide Actinide Res.*, submitted for publication.